Chaos induced by quantum effect due to breakdown of the Born-Oppenheimer adiabaticity

Hiroshi Fujisaki* and Kazuo Takatsuka†
Department of Basics Science, Graduate School of Arts and Sciences, University of Tokyo, 153-8902, Tokyo, Japan
(Received 1 December 2000; published 29 May 2001)

Chaos in the multimode nonadiabatic system constructed by Heller [J. Chem. Phys. **92**, 1718 (1990)], which consists of two diabatic two-dimensional harmonic potentials with the Condon coupling, is studied. A thorough investigation is carried out by scanning the magnitudes of the Condon coupling and the Duschinsky angle. To elucidate mechanisms that can cause chaos in this quantum system, the statistical properties of the energy levels and eigenfunctions of the system are investigated. We find an evidence in terms of the nearest-neighbor spacing distribution of energy levels and other measures that a certain class of chaos is *purely* induced by the nonadiabatic interaction due to breakdown of the Born-Oppenheimer approximation. Since the nonadiabatic transition can induce repeated bifurcation and merging of a wave packet around the region of quasicrossing between two potential surfaces, and since this interaction does not have a counterpart in the lower adiabatic system, the present chaos deserves being called ''nonadiabatic chaos.'' Another type of chaos in a nonadiabatic system was previously identified [D. M. Leitner *et al.*, J. Chem. Phys. **104**, 434 (1996)] that reflects the inherent chaos of a corresponding adiabatic potential. We present a comparative study to establish the similarity and difference between these kinds of chaos.

DOI: 10.1103/PhysRevE.63.066221 PACS number(s): 05.45.Mt, 34.10.+x, 34.30.+h, 34.70.+e

I. INTRODUCTION

Quantum chaos has long been a controversial subject in physics [1] in that it is extremely difficult to define chaos in the Schrödinger linear equation in a convincing way. Nonetheless one often observes complexity in quantum phenomena such as in spectral features, eigenfunctions, and dynamics in molecular processes, solid-state physics, nuclear physics, and so on. The most widely accepted terminology alternative to ''quantum chaos'' is ''quantum chaology'' due to Berry [2] , which is meant as a quantum or semiclassical study of a system whose classical counterpart exhibits chaos. Despite the clear definition of quantum chaology, ''quantum chaos'' is quite often used as a synonym of it. Many intriguing facts have been found in quantum chaological systems: they often have the Wigner-type nearest-neighbor spacing distribution of energy eigenvalues, whereas integrable systems show the Poisson-type distribution [1–3]. Contrary to Berry's statistical argument [4], Heller found some highly excited states in a quantum chaos system to localize spatially along classical *unstable* periodic orbits, which is called ''scars'' [5]. Deterministic diffusion in a classical chaotic system is often suppressed in the corresponding quantum chaos system [6]. The curious relationship between quantum tunneling and chaos [7–10] is another topic. The semiclassical quantization of energy levels mainly based on the Gutzwiller's trace formula [1,11] and the Fourier transformation of the time-correlation function [12,13] remain among the most difficult subjects in the study of chaos.

On the other hand, there are quantum systems that do not have a naive classical counterpart, and even in such systems one can expect chaotic phenomena. For example, several authors have studied ''chaos'' in spin-boson models [14–16]. These models are related to many realistic physical systems, e.g., micromasers [17], mesoscopic magnets [18], electron-transfer systems [19], etc., and while an understanding of these models can hence have many practical implications, their chaotic aspects are not well understood.

We have been studying chaos in a nonadiabatic system due to breakdown of the Born-Oppenheimer approximation, in which two or more potential functions are coupled through a nonadiabatic interaction. Since a wave packet placed on one of the potential surfaces can undergo repeated bifurcation and merging around their quasicrossing region, one can (naively) expect ''chaos'' to occur. This kind of complicated wave packet motion has been theoretically observed even in one-dimensional nonadiabatic systems such as electron transfer in NaI molecule, which can be expected to be observed experimentally via the pump-probe femtosecond photoelectron spectroscopy [20]. Although the present study is motivated by the multidimensional or multimode effects in electron transfer in molecular systems, our report is concerned with a rather general and simplified scheme to investigate common underlying features of those systems. To this aim, we study a simple system that was proposed by Heller [21], which can be regarded as a simple model for the above-listed systems by rewriting them in a spin-boson model. The Heller system consists of two-dimensional, two diabatic *harmonic* potentials, which are nonadiabatically coupled under the Condon approximation. We call it a *two-mode-two-state* (TMTS) system [22].

Heller stated in his study on his own system that ''the hopping from one energy surface to another is enough to cause classical chaos and strong mixing of the levels quantum mechanically.'' He actually has shown that his system exhibits chaotic properties in terms of his spectral measure [23]. Although his argument is clear and sound, there remains a highly nontrivial question about the mechanism of ''chaos'' in the nonadiabatic system (see a paragraph below the next one).

*Email address: fujisaki@mns2.c.u-tokyo.ac.jp
†Email address: kaztak@mns2.c.u-tokyo.ac.jp

 ©2001 The American Physical Society

In a previous paper, we studied highly excited eigenfunctions in the TMTS system with Heller's ''chaos'' values of the system parameters [22]. In the study, among rather characterless ''chaotic'' eigenfunctions that are uniformly widespread in configuration space, we have found two extreme types of the eigenfunctions that favor to localize either on the diabatic surface or the adiabatic surface. It also has been shown that the behavior of nonadiabatic transition depends strongly on the locations where an initial wave packet is prepared, reflecting the properties of the localized eigenfunctions. This fact in turn can provide a guiding principle to control the rate of electron transfer by using laser techniques or by choosing appropriate solvents.

In this paper, we concentrate on the more chaotic aspect of this nonadiabatic system. There can be two types of chaos that may occur in a nonadiabatic system; (1) chaos directly reflecting the chaos on the adiabatic potential surface and (2) chaos that is induced by the very nonadiabatic interaction itself. The former has already been identified by Leitner *et al*. using Jahn-Teller molecules [24]. To identify the latter class, we compare the nonadiabatic system with the corresponding lower adiabatic system from *statistical* points of view by systematically scanning the values of the nonadiabatic coupling constant and the Duschinsky angle. The measures we employ are rather popular ones; the nearest-neighbor spacing distribution (NNSD) of energy levels [3], Δ_3 statistic of Dyson and Mehta [3] (or called spectral rigidity [11]) and the amplitude distribution of the eigenfunctions [4,25]. Here we show a numerical evidence of the existence of the second class of chaos. This chaos is really intrinsic to nonadiabaticity in that no classical chaos can play a role.

This paper is organized as follows: In Sec. II, we describe Heller's TMTS system and the numerical procedures to obtain the energy levels and eigenfunctions of the system. In Sec. III , we investigate the statistical properties of the energy levels and eigenfunctions of the system. In Sec. IV, the corresponding properties of the lower adiabatic system are examined. In Sec. V, we summarize the paper, identifying the nonadiabatic chaos.

II. HELLER'S TMTS SYSTEM AND NUMERICAL PROCEDURES

We now introduce Heller's TMTS system along with our numerical procedure to obtain the energy spectrum. The starting Hamiltonian is (see Fig. 1)

$$\mathcal{H}=\begin{pmatrix} T_{\rm kin}+V_A & J \\ J & T_{\rm kin}+V_B \end{pmatrix}, \tag{1}$$

where

$$T_{\rm kin}=\frac{1}{2}(p_x^2+p_y^2), \quad V_i=\frac{1}{2}(\omega_x^2\xi_i^2+\omega_y^2\eta_i^2)+\epsilon_i \quad (i=A,B) \tag{2}$$

with

$$\xi_A=x\cos\theta-(y-a)\sin\theta, \quad \eta_A=x\sin\theta+(y-a)\cos\theta, \tag{3}$$

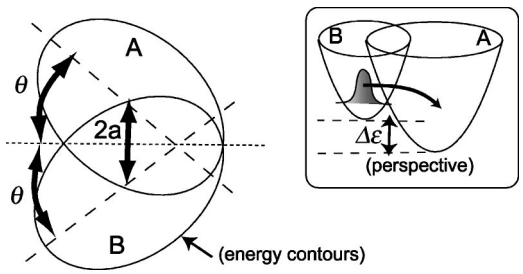

FIG. 1. A schematic representation of Heller's TMTS system. The distance between the centers of the potentials is $2a$, and the angle between the relevant crossing seam (dotted line) and the primary axis of each potential (dashed line) is θ. Inset: The perspective of the TMTS system. The desymmetrization is represented by the difference of the energy minima: $\Delta\epsilon=\epsilon_B-\epsilon_A$.

$$\xi_B=x\cos\theta+(y+a)\sin\theta, \quad \eta_B=-x\sin\theta+(y+a)\cos\theta. \tag{4}$$

Note that this is different from our previous choice of the coordinates [22], and is the same as Heller's: $T_{\rm kin}$ is a nuclear kinetic energy, V_i $(i=A,B)$ diabatic potentials of each electronic state i, J the nonadiabatic coupling constant between the electronic states, and ϵ_i $(i=A,B)$ the energy minima of the potentials. The geometrical meanings of a and θ are illustrated in Fig. 1. A nonvanishing θ, which corresponds to the so-called Duschinsky angle [26], causes a complicated coupling between x and y (Duschinsky effects). The relevant crossing seam is denoted by a dotted line in Fig. 1. In this coordinate system, it is approximately given by $y=0$. (See also [22].)

To obtain the energy levels and eigenfunctions of the TMTS system, we directly diagonalize the Hamiltonian of the system. To this end, we first unitarily transform $\mathcal{H}$ with

$$U=\frac{1}{\sqrt{2}}\begin{pmatrix} 1 & 1 \\ -1 & 1 \end{pmatrix}$$

such that

$$\tilde{\mathcal{H}}=U^\dagger\mathcal{H}U=\begin{pmatrix} T_{\rm kin}+V_+-J & V_- \\ V_- & T_{\rm kin}+V_++J \end{pmatrix}, \tag{5}$$

where $V_\pm=(V_A\pm V_B)/2$ are explicitly given by

$$V_+=\frac{1}{2}\tilde{\omega}_x^2(x-\tilde{a})^2+\frac{1}{2}\tilde{\omega}_y^2y^2-\frac{1}{2}\tilde{\omega}_x^2\tilde{a}^2+\frac{1}{2}\tilde{\omega}_y^2a^2+\frac{\epsilon_A+\epsilon_B}{2}, \tag{6}$$

$$V_-=(\Delta\omega)^2xy-\tilde{\omega}_y^2ay+\frac{\epsilon_A-\epsilon_B}{2}, \tag{7}$$

and

$$\tilde{\omega}_x^2=\omega_x^2\cos^2\theta+\omega_y^2\sin^2\theta, \quad \tilde{\omega}_y^2=\omega_x^2\sin^2\theta+\omega_y^2\cos^2\theta,$$

$$(\Delta\omega)^2=(\omega_y^2-\omega_x^2)\cos\theta\sin\theta, \quad \tilde{a}=\frac{(\Delta\omega)^2}{\tilde{\omega}_x^2}a.$$

Now we define the eigenstates of $T_{\rm kin}+V_+$ as $|n_x,n_y\rangle$, i.e.,

$$(T_{\rm kin}+V_+)|n_x,n_y\rangle = E_{n_x,n_y}|n_x,n_y\rangle, \tag{8}$$

$$E_{n_x,n_y} = \hbar\tilde{\omega}_x(n_x+1/2)+\hbar\tilde{\omega}_y(n_y+1/2). \tag{9}$$

We also define electronic states that rotate the diabatic states $|i\rangle$ $(i=A,B)$ by $U^\dagger$, i.e.,

$$|1\rangle\!\rangle \equiv U^\dagger|A\rangle = (|A\rangle+|B\rangle)/\sqrt{2}, \tag{10}$$

$$|2\rangle\!\rangle \equiv U^\dagger|B\rangle = (-|A\rangle+|B\rangle)/\sqrt{2}. \tag{11}$$

Then, by taking the direct product of $|n_x,n_y\rangle$ and $|i\rangle\!\rangle$ $(i=1,2)$ as a basis set to express the Hamiltonian, we obtain the matrix elements analytically as

$$\begin{aligned}\langle n_x,n_y|H_{11}|n_x',n_y'\rangle &= \langle n_x,n_y|T_{\rm kin}+V_+-J|n_x',n_y'\rangle \\ &= (E_{n_x,n_y}+\epsilon_+)\,\delta_{n_x,n_x'}\delta_{n_y,n_y'},\end{aligned} \tag{12}$$

$$\begin{aligned}\langle n_x,n_y|H_{22}|n_x',n_y'\rangle &= \langle n_x,n_y|T_{\rm kin}+V_++J|n_x',n_y'\rangle \\ &= (E_{n_x,n_y}+\epsilon_-)\,\delta_{n_x,n_x'}\delta_{n_y,n_y'},\end{aligned} \tag{13}$$

$$\begin{aligned}\langle n_x,n_y|H_{12}|n_x',n_y'\rangle &= \langle n_x,n_y|V_-|n_x',n_y'\rangle \\ &= [c_1\delta_{n_x,n_x'}+c_2(\sqrt{n_x+1}\,\delta_{n_x,n_x'-1} \\ &\quad +\sqrt{n_x}\,\delta_{n_x,n_x'+1})](\sqrt{n_y+1}\,\delta_{n_y,n_y'-1} \\ &\quad +\sqrt{n_y}\,\delta_{n_y,n_y'+1}) \\ &\quad +\frac{\epsilon_A-\epsilon_B}{2}\delta_{n_x,n_x'}\delta_{n_y,n_y'},\end{aligned} \tag{14}$$

where $H_{ij}=\langle\!\langle i|\mathcal{H}|j\rangle\!\rangle$ $(i,j=1,2)$, $\delta_{n,m}$ is the Kronecker delta function, and

$$\epsilon_\pm = -\frac{1}{2}\tilde{\omega}_x^2\tilde{a}^2+\frac{1}{2}\tilde{\omega}_y^2a^2+\frac{\epsilon_A+\epsilon_B}{2}\mp J,$$

$$c_1=[(\Delta\omega)^2\tilde{a}-\tilde{\omega}_y^2a]\sqrt{\frac{\hbar}{2\tilde{\omega}_y}}, \quad c_2=\frac{\hbar(\Delta\omega)^2}{2\sqrt{\tilde{\omega}_x\tilde{\omega}_y}}.$$

We have confirmed convergence of the results by changing the size of the basis set. (Around $E=29$, we need a $\sim 7000\times 7000$ matrix to achieve converged results if the system is ''chaotic.'') We also used the screening method [27,22] to cross check some of the results, and we have demonstrated the convergence of the lowest 1200 eigenenergies to at least five significant digits.

The lower adiabatic system is defined by the Hamiltonian $T_{\rm kin}+V_{\rm ad}^-$ where $V_{\rm ad}^-=V_+-\sqrt{V_-^2+J^2}$. Thus we again use the eigenstates of the Hamiltonian $T_{\rm kin}+V_+$ as the basis set to represent the matrix elements. For efficient computation of the matrix elements, we have used the Gauss-Hermite quadrature [28]. Nevertheless, this integration is time consuming, and hence the computational time is much longer than in the case of the nonadiabatically coupled system. Again, we have used the screening method to cross check some of the results.

TABLE I. System parameters.

$\hbar$	ω_x	ω_y	a	ϵ_A	ϵ_B
1.0	0.8716	1.1725	3.0	0.0	0.173

Finally, the system parameters adopted throughout this paper are listed in Table I. In order to study how chaos can appear generally in nonadiabatic systems, we scan the values of J (nonadiabaticity) and θ (Duschinsky angle) to see its consequence in the statistical properties of the system. Heller's system with two (vibrational) modes and two (electronic) states is a minimal model for this purpose. To our best knowledge, there has been no work of this kind in the past. The systematic survey in the present approach should also be quite useful for our future study of control of nonadiabatic systems by means of varying solvents and/or applying external fields [29].

III. STATISTICAL PROPERTIES OF THE NONADIABATICALLY COUPLED SYSTEM

A. Statistics of the energy levels

The NNSD of energy levels is one of the established measures to identify chaos in nuclear physics and molecule physics. The NNSD's of model systems (e.g., billiard systems [2,3]), and realistic systems (e.g., triatomic molecules [30]) have been examined in the past, and it has been established that the NNSD of a quantum system usually becomes the Wigner type

$$P(S)=\frac{\pi}{2}S\exp\left\{-\frac{\pi}{4}S^2\right\}, \tag{15}$$

if the corresponding classical system is chaotic with time-reversal symmetry. Hereafter we approximately call this type the Gaussian-orthogonal ensemble (GOE) type. On the other hand, the NNSD of a quantum system usually becomes the Poisson type

$$P(S)=\exp\{-S\} \tag{16}$$

if the corresponding classical system is integrable. While the NNSD measures a short-range correlation among the energy levels, the Δ_3 statistic (spectral rigidity) is designed to detect a long-range correlation among them [3]. The latter is defined by

$$\Delta_3(E,L)=\min_{A,B}\frac{1}{L}\int_{E-L/2}^{E+L/2}[\hat{N}(x)-Ax-B]^2\,dx, \tag{17}$$

where $\hat{N}(x)$ is the unfolded cumulative level density of the system considered [3]. The average of $\Delta_3(E,L)$ over the energy, which is denoted by $\overline{\Delta_3}(L)$, of a quantum system usually behaves like

$$\overline{\Delta}_3(L) = \frac{1}{\pi^2}(\ln L - 0.068), \tag{18}$$

if the corresponding classical system is chaotic with time-reversal symmetry. This form can also be derived from the GOE [3]. On the other hand, $\overline{\Delta}_3(L)$ of a quantum system usually behaves like

$$\overline{\Delta}_3(L) = \frac{L}{15} \tag{19}$$

when the corresponding classical system is integrable.

Since the nonadiabatic system as well as the other spin-boson models have no naive classical counterpart, application of these measures would be doubtful even if they are well established in quantum chaology. Nevertheless, the NNSD's have been calculated for many other nonadiabatic systems successfully: Cederbaum and co-workers [31] studied Jahn-Teller molecules that have conical intersections and found that the NNSD for NO_2 is of the GOE type whereas that for $C_2H_4^+$ has a 'mixed' character between the GOE type and the Poisson type. Their model systems have *three* vibrational modes and *two* electronic states. On the other hand, Kuś showed that a simple spin-boson model which has *one* (vibrational) mode and *two* (electronic) states does not exhibit any universal character in the NNSD [32]. After the work of Kuś, Graham and Höhnerbach investigated a similar spin-boson model with more numbers of spins, and found that the NNSD approaches the GOE type even with one (vibrational) mode [33]. Their system is considered as a nonadiabatic system with *one* vibrational mode and *many* electronic states, it is hence interesting to apply the statistical measure to the Heller system with *two* vibrational modes and *two* electronic states.

Some notes: We did not desymmetrize the system in case of $\theta = 0$ and $\pi/2$, and therefore the system has a reflection symmetry with respect to the *y* axis. We have confirmed that desymmetrization changes the results only slightly. To calculate the NNSD's and the Δ_3 statistics, we unfold the energy levels between $E \simeq 25$ and $E \simeq 35$ (about 600 levels were included) using a third-order polynomial fitting for the cumulative level density [31]. In this paper, we do not use any interpolating formulas like the Brody [34], or the Berry-Robnik [24] distributions. The results with increasing strength of the nonadiabatic coupling *J* are shown in Figs. 2, 3, and 4, which are discussed below.

1. Weak coupling case

First we investigate the case $J = 0.3$, which is classified as a weak coupling (diabatic) case in the sense that $J < \hbar\omega_x, \hbar\omega_y$. In this case, the energy-level statistics for the system show the anomalous behavior of the *harmonic limit* [35] because the system consists of nearly uncoupled harmonic oscillators. To eliminate this nongeneric effect, we add the fourth order terms to the diabatic potentials

$$\Delta V_i = \frac{\alpha_x}{4}\xi_i^4 + \frac{\alpha_y}{4}\eta_i^4 \quad (i = A, B), \tag{20}$$

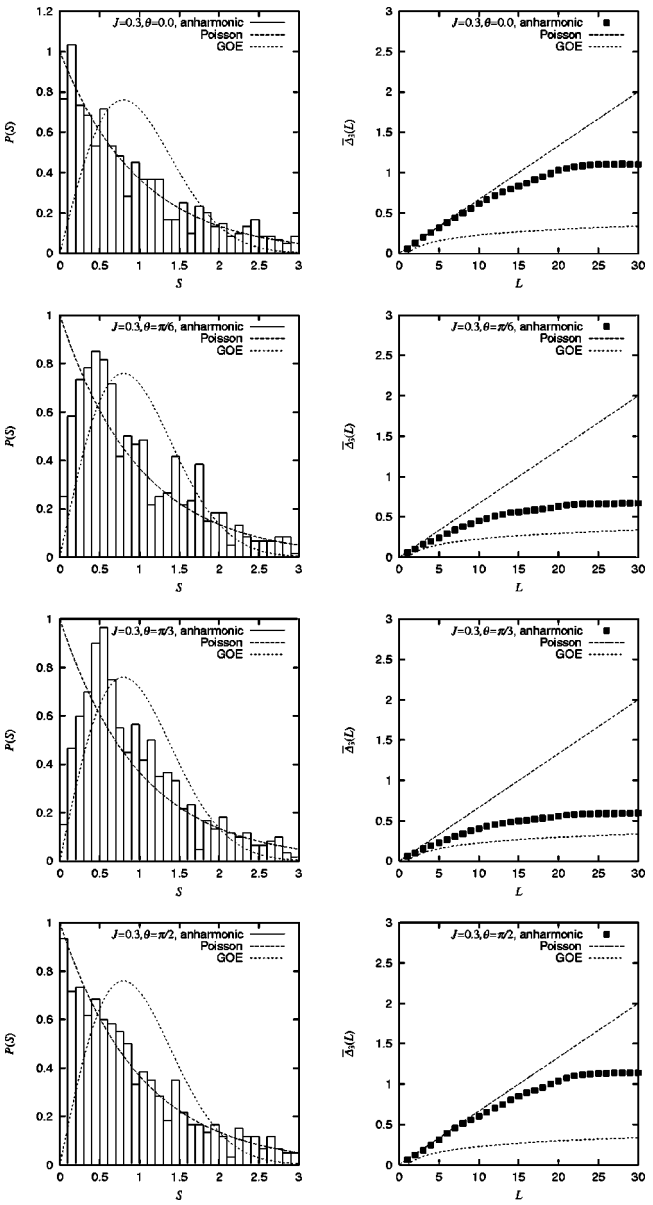

FIG. 2. Left column: NNSD's of Heller's TMTS system with $J = 0.3$ (weak coupling) and weak anharmonicity. From top to bottom, $\theta = 0.0$, $\pi/6$, $\pi/3$, and $\pi/2$. Right column: The corresponding Δ_3 statistics.

where ξ_i and η_i have been defined in Eqs. (3) and (4), and α_x and α_y represent the strength of nonlinearity. Note that addition of these terms does not induce any chaos in the diabatic systems because the variables are separable. The values of nonlinearity are taken as $\alpha_x = 0.001, \alpha_y = 0.0012$, which bring about a few percent energy-level difference. Nonetheless, it makes the energy-level statistics more generic and natural. See Fig. 2: The NNSD's for $\theta = 0$ and $\pi/2$ appear to be clear Poisson distributions. Each of the skewed systems with $\theta = \pi/6$ and $\pi/3$ shows a clear hole at $S = 0$, although they are not a clear GOE (Wigner) type. For the other cases discussed below (the intermediate and strong coupling cases), the inclusion of the nonlinearity does not qualitatively change the results [29], so the calculations below are performed with the original harmonic potentials.

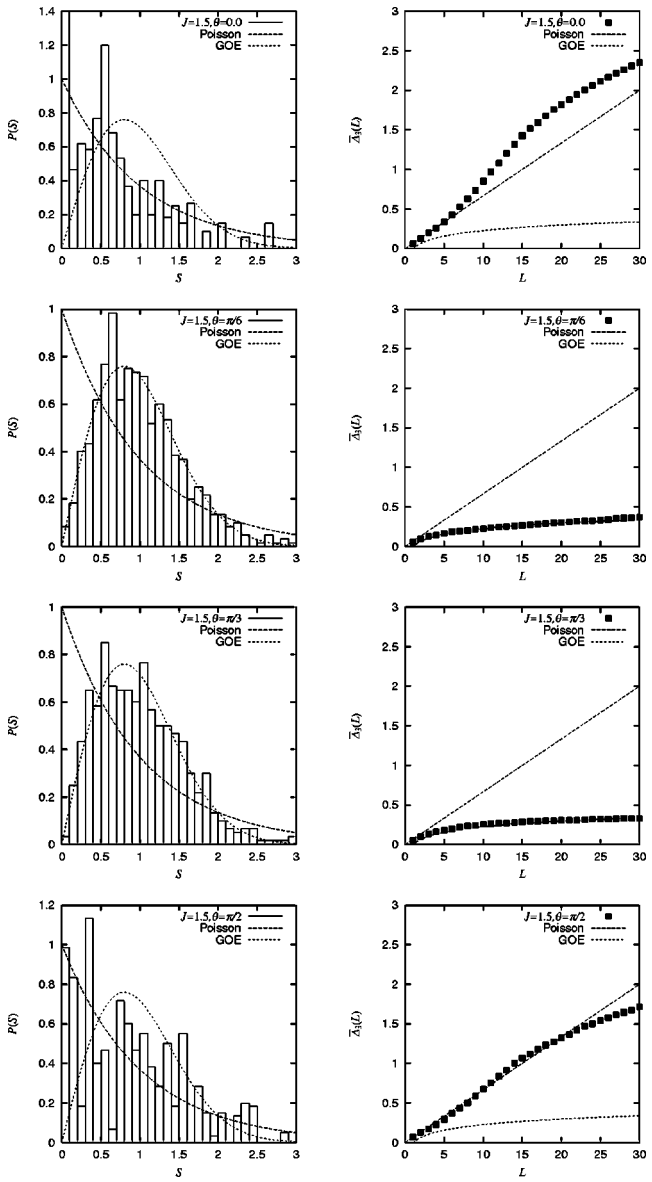

FIG. 3. Left column: NNSD's of Heller's TMTS system with $J=1.5$ (intermediate coupling). From top to bottom, $\theta=0.0$, $\pi/6$, $\pi/3$, and $\pi/2$. Right column: The corresponding Δ_3 statistics.

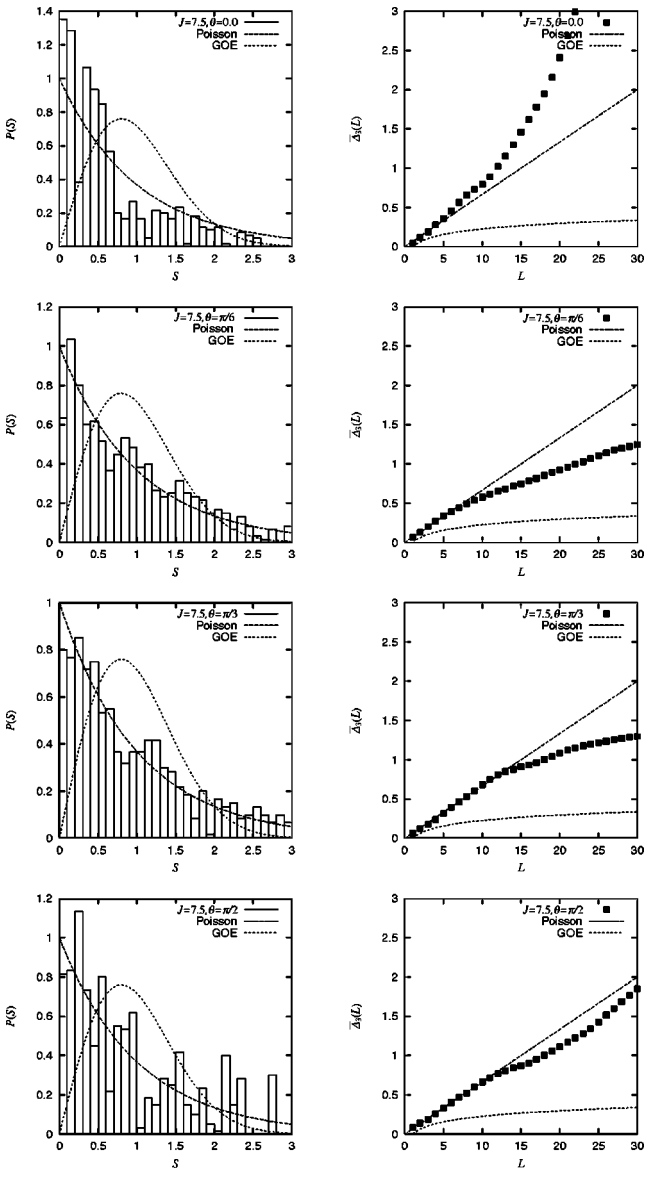

FIG. 4. Left column: NNSD's of Heller's TMTS system with $J=7.5$ (strong coupling). From top to bottom, $\theta=0.0$, $\pi/6$, $\pi/3$, and $\pi/2$. Right column: The corresponding Δ_3 statistics.

2. Intermediate coupling case

Next we investigate the intermediate coupling case, i.e., $J=1.5\sim\hbar\omega_x,\hbar\omega_y$. (This is Heller's ''chaos'' value [21].) From Fig. 3, when the Duschinsky angle has intermediate values, i.e., $\theta=\pi/6$ or $\theta=\pi/3$, this TMTS system shows the typically quantum chaotic behavior both in the NNSD and Δ_3 statistics [see Eqs. (15) and (18)]. This is consistent with the statement of Heller based on his own spectral criterion [21]. Heller's criterion of chaos measures an averaged property of eigenfunctions, while the NNSD and Δ_3 statistic address the statistical properties of energy levels. Thus the present intermediate coupling system has been confirmed to be chaotic in these aspects.

3. Strong coupling case

We further proceed to the strong coupling (adiabatic) case, i.e., $J=7.5>\hbar\omega_x,\hbar\omega_y$. From Fig. 4, we clearly see the level clustering and the Poisson trend, especially, for $\theta=\pi/6$ or $\theta=\pi/3$. However, the Δ_3 statistics deviate from the straight line [Eq. (19)] for large L values. Except for the case $\theta=0$, the Δ_3 statistics have lower values than Eq. (19) and approach Eq. (18). This might reflect the mixed (tori + stochastic seas) structure of the lower adiabatic system and suggests the use of some interpolating formulas. Thus the strong coupling case shows mostly a regular spectrum when judged by the energy-level statistics. It thus turns out that the chaoticity of the system is not simply monotonic with respect to the magnitude of the coupling parameter J, although it leads the system to deviate from the harmonic state and to approach a more adiabatic-favored and anharmonic situation. Thus, we need to clarify the nature of the dynamics on the corresponding adiabatic state. We will come back to this issue in the next section.

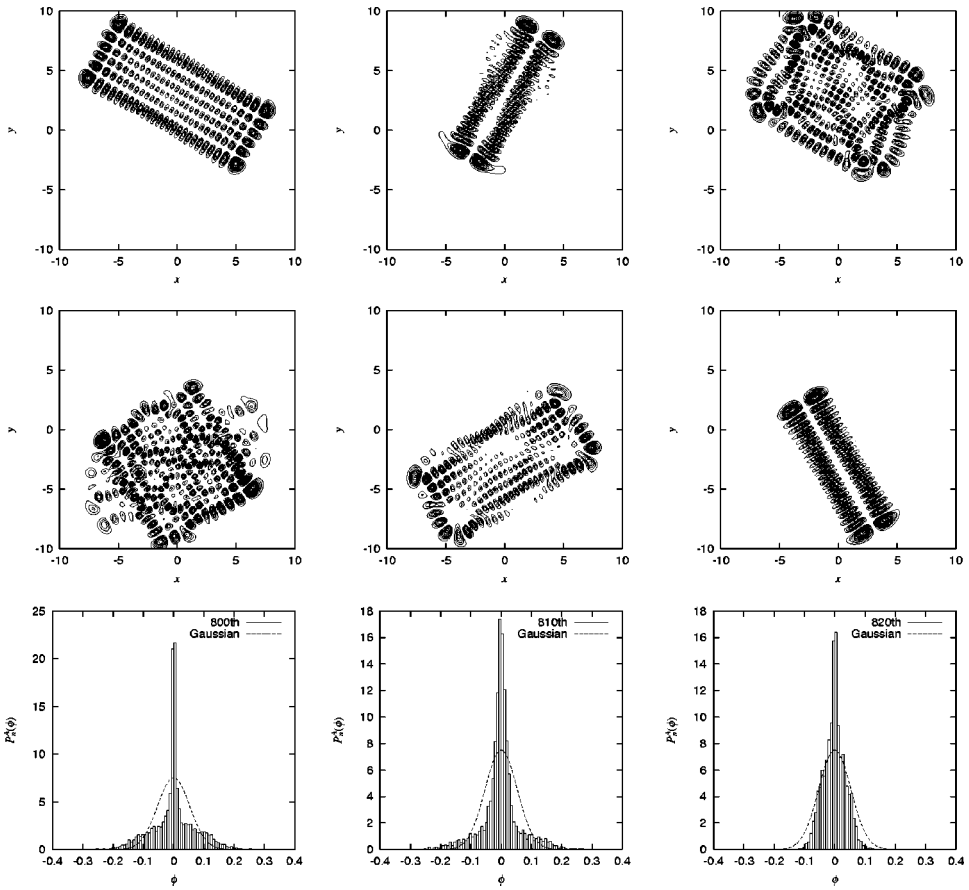

FIG. 5. First row: Eigenfunctions squared (from left to right, 800th, 810th, and 820th) of Heller's TMTS system on surface A with $J=0.3$ (weak coupling) and $\theta=\pi/6$. Second row: The corresponding eigenfunctions (squared) on surface B. Third row: The corresponding amplitude distributions of the eigenfunctions on surface A. The dashed line represents the Gaussian with width $\sigma=0.053$.

B. Amplitude distributions of the eigenfunctions

In this section we investigate a statistical property of the eigenfunctions, namely, the amplitude distribution [4,25]. The amplitude distribution for the nth eigenfunction on surface i $(i=A,B)$, denoted by $P_n^i(\phi)$, is defined by the frequency distribution of the amplitude (ϕ) of the eigenfunction that is randomly sampled at points that are energetically accessible in configuration space. We actually take ~ 6000 points.

According to Berry [4], the histogram of $P_n^i(\phi)$ should reflect the chaotic property of an eigenfunction. He conjectured that the amplitude distribution for a classically chaotic system should become a Gaussian distribution,

$$P(\phi)=\frac{1}{\sqrt{2\pi\sigma^2}}\exp\left\{-\frac{\phi^2}{2\sigma^2}\right\}, \tag{21}$$

with the width $\sigma=1/\sqrt{S}$ where S is the area of the energetically accessible region. This is called Berry's criterion of ''chaos'' for eigenfunctions, and has been tested successfully in the literature [25]. In case of a single surface with a potential $V(x,y)$, the area S is easily identified; it is the area enclosed by a curve (x,y) satisfying $V(x,y)=E$. However, in case of coupled surfaces as in our nonadiabatic system, the meaning of S is not necessarily clear. In this paper, we suggest using the sum of the areas enclosed by $V_i(x,y)=E$ on each diabatic surface. That is, each surface has the area $\sim 2\pi E/\omega_x\omega_y$, then the width is expected to be

$$\sigma\simeq\sqrt{\frac{\omega_x\omega_y}{4\pi E}}\simeq 0.053, \tag{22}$$

where we have used $E\simeq 29$ that is the energy of interest. The results for $P_n^A(\phi)$ are shown in the third rows of Figs. 5, 6, and 7 with the corresponding eigenfunctions on the diabatic surfaces (first and second rows). In terms of this criterion, let us examine selected eigenfunctions: 800th, 810th and 820th with $\theta=\pi/6$ for each coupling strength $J=0.3$, 1.5, and 7.5. Their energies are around $28-29$, which are much higher than the bottle-neck energy of the lower adiabatic surface ~ 4.7.

1. Weak coupling case

In Fig. 5, we can see that the amplitude distributions are more or less different from the Gaussian, Eq. (21), with the width, Eq. (22). These eigenfunctions have rather clear nodal patterns that can be easily counted. Hence these amplitude distributions are far from chaos. Since there are many empty regions inside the equienergy contour, their amplitude distributions concentrate at $\phi=0$. The top-right figure of Fig. 5 seems a little ''disordered,'' but the amplitude distribution still deviates from the Gaussian. Thus these eigenfunctions turn out to be nonchaotic.

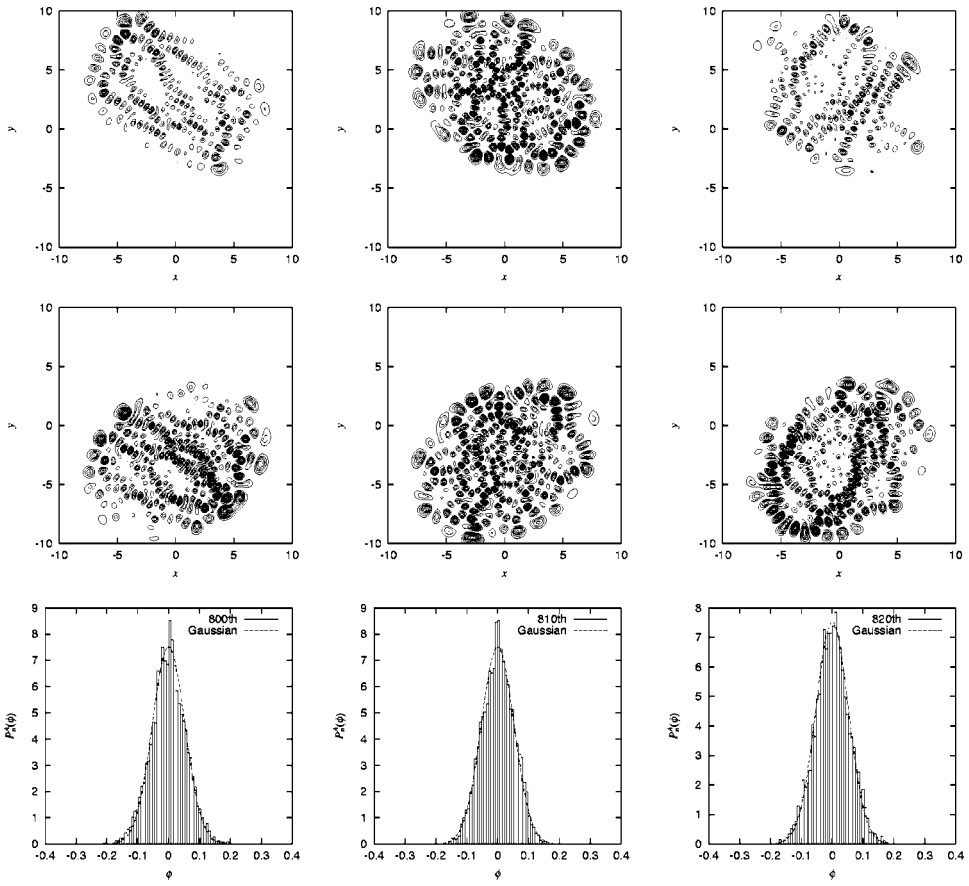

FIG. 6. First row: Eigenfunctions squared (from left to right, 800th, 810th, and 820th) of Heller's TMTS system on surface A with $J=1.5$ (intermediate coupling) and $\theta=\pi/6$. Second row: The corresponding eigenfunctions (squared) on surface B. Third row: The corresponding amplitude distributions of the eigenfunctions on surface A. The dashed line represents the Gaussian with width $\sigma=0.053$.

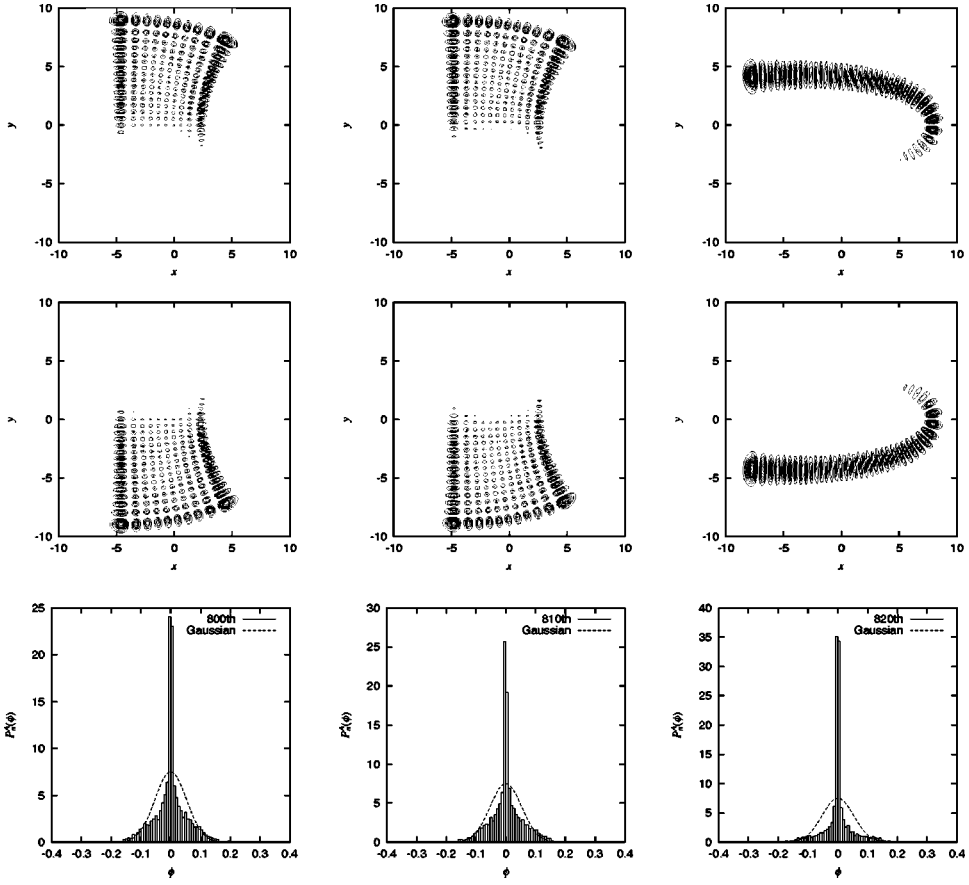

FIG. 7. First row: Eigenfunctions squared (from left to right, 800th, 810th, and 820th) of Heller's TMTS system on surface A with $J=7.5$ (strong coupling) and $\theta=\pi/6$. Second row: The corresponding eigenfunctions (squared) on surface B. Third row: The corresponding amplitude distributions of the eigenfunctions on surface A. The dashed line represents the Gaussian with width $\sigma=0.053$.

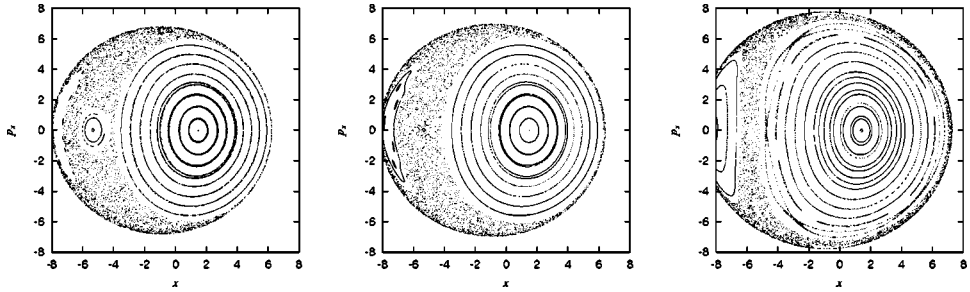

FIG. 8. Poincaré surfaces of section for the lower-adiabatic system ($E=28$). The nonadiabatic coupling is $J=0.3$ (left), 1.5 (middle), and 7.5 (right). The Duschinsky angle is $\theta=\pi/6$.

2. Intermediate coupling case

From Fig. 6, we can clearly see that the amplitude distributions with a variety of energies are very similar to the Gaussian. Therefore, according to Berry's criterion, the system with the above choice of parameters is well ''quantum chaotic.'' This result reinforces Heller's conclusion [21] based on his spectral criterion [23] . (Note, however, that the spectral criterion uses only an *averaged* property of eigenfunctions.) Thus it turns out that the intermediate coupling case is an undisputed chaos by any statistical measure.

3. Strong coupling case

The strong coupling case (Fig. 7) is in a sense similar to the weak coupling case: the amplitude distributions more or less deviate from the Gaussian. All these figures exhibit clear nodal patterns that can be easily counted. In fact, we can see that left two are confined in a torus whereas the right most is confined in another torus. Though not shown here, this can be clearly confirmed if one uses the adiabatic representation.

IV. STATISTICAL PROPERTIES OF THE LOWER ADIABATIC SYSTEM

A. Poincaré surface of section

To identify and distinguish two types of chaos in nonadiabatic systems as stated in the Introduction, namely, chaos of a direct reflection of that on the adiabatic potential surface and intrinsic chaos purely induced by the nonadiabatic interaction, a comparative study of dynamics on the corresponding adiabatic system is inevitable. We here study the J dependence of the lower adiabatic system fixing $\theta=\pi/6$.

The classical Poincaré surfaces of section at the crossing seam ($y=0$) are drawn in Fig. 8 [22]. It turns out that the ratio of chaotic sea to tori (stable area) does not change drastically with J, and that the area of the latter is rather wider than that of the former. Thus, it is highly expected [24] that none of the forecasted NNSD's should be similar to the GOE type in contrast to the case of the full coupled system with $J=1.5$. We next confirm this by actually calculating the statistical properties of the energy levels and eigenfunctions on the lower adiabatic potentials.

B. Statistics for the energy levels

The NNSD's and Δ_3 statistics are shown in Fig. 9. Both of these measures suggest that the level statistics are basically ''regular.'' Following the tentative argument using the Berry-Robnik distribution [24], the chaos-tori ratio is nearly equal to the Berry-Robnik parameter q, and this implies, in this case, that the NNSD's are rather similar to the Poisson type. We recall that the nonadiabatic system with $J=7.5$ (strong coupling) is mostly regular in the energy-level statistics. This is presumably so because the strong coupling case is close to the adiabatic limit and the dynamics on the nonadiabatic system should be dominated by that on the corre-

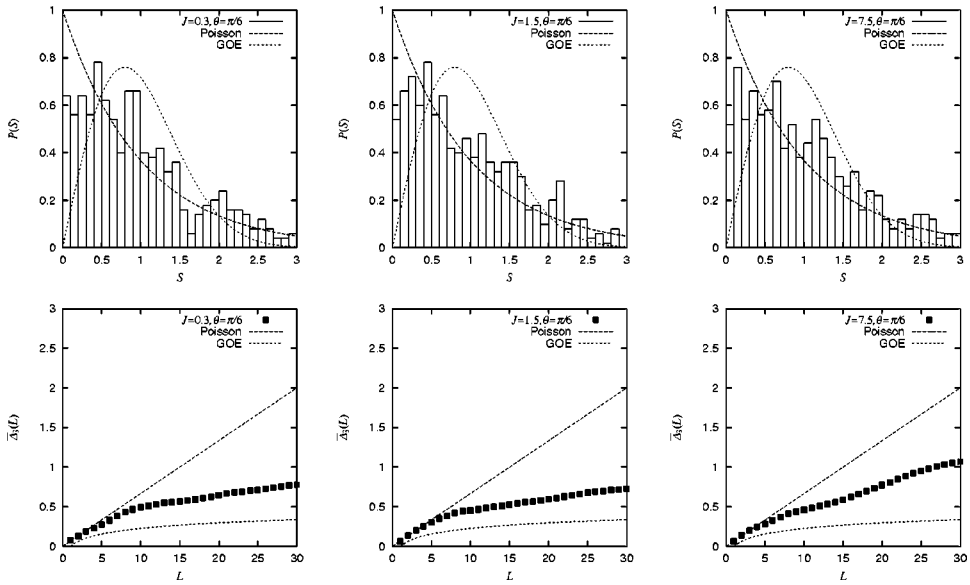

FIG. 9. First row: NNSD's of the lower adiabatic system. From left to right, $J=0.3$, 1.5, and 7.5 while fixing $\theta=\pi/6$. Second row: The corresponding Δ_3 statistics.

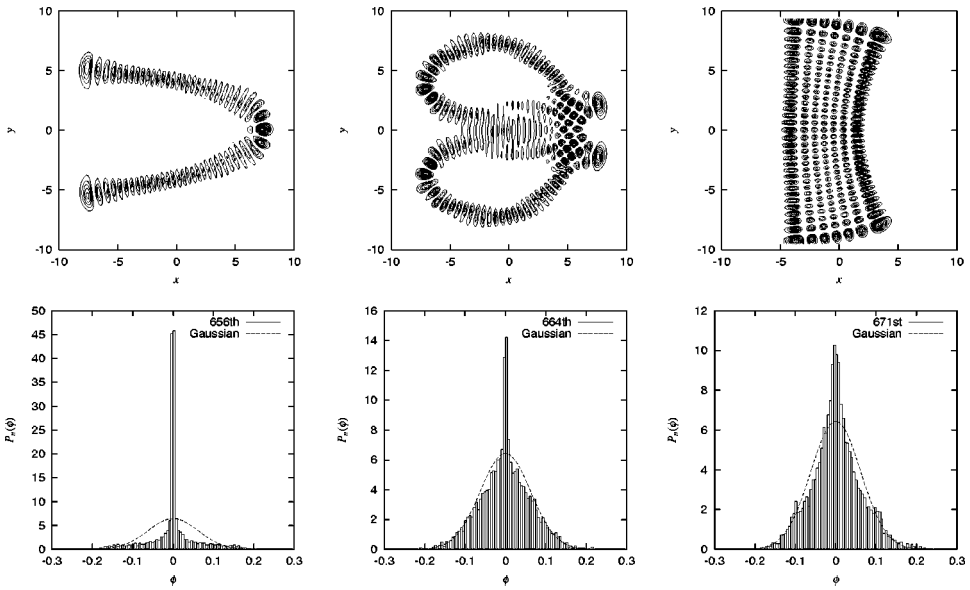

FIG. 10. First row: Eigenfunctions squared (from left to right, 656th, 664th, and 671st) of the lower adiabatic system with $J=1.5$ and $\theta=\pi/6$. Second row: The corresponding amplitude distributions. The dashed line represents the Gaussian with width $\sigma=0.062$.

sponding adiabatic potential surface. In fact, the measures for the adiabatic and nonadiabatic cases with $J=7.5$ are similar.

C. Amplitude distributions of the eigenfunctions

Selected eigenfunctions (656th, 664th, and 671st) of the lower adiabatic system with $J=1.5$ and $\theta=\pi/6$ are shown in Fig. 10 with the associated amplitude distributions. Note that, in this case, we take $\sigma=0.062$ because the area enclosed by the equienergy contour with $E\simeq 28$, which is the energy of interest, is $\simeq 260$. As are the cases of Figs. 5 and 7, these amplitude distributions deviate more or less from the Gaussian, indicating a nonchaotic feature. This is consistent with the level statistics shown in the middle figures of Fig. 9. Note that these parameter values induced strongly chaotic features in the corresponding nonadiabatic system. Nevertheless, the eigenfunctions on the adiabatic potential surface for this case are mostly regular in the energy range studied. This is due to the ''quantum smoothing'' effect [36], and it might be said, in turn, that nonadiabaticity breaks the quantum smoothing effect.

V. SUMMARY

The statistical properties for the nonadiabatic and the corresponding adiabatic systems we have numerically observed are summarized in Table II. We thus conclude that the chaos in the nonadiabatic system with the intermediate coupling ($J=1.5$) and the intermediate Duschinsky angle (e.g., $\theta=\pi/6$) has been induced purely by the nonadiabatic coupling, which is peculiar to quantum mechanics. Leitner *et al.* made an extensive study to compare nonadiabatic systems (Jahn-Teller molecules) with their adiabatic counterparts (the lower adiabatic systems) [24]. They say that ''most of the *irregularity* in the full spectra arises from the irregularity in the spectra obtained using the adiabatic potential.'' The case investigated by Leitner *et al.* might be quite universal and natural for JT molecules. On the other hand, the chaos in our nonadiabatic system is not a simple reflection of chaos on the lower adiabatic potential surface nor that on the diabatic surface (the diabatic surface is a harmonic potential). We can draw this conclusion from the fact that the adiabatic case (the middle of Fig. 9) indicates rather Poisson trends for both measures (the Δ_3 statistic is along the Poisson line until $L\simeq 5$), whereas the nonadiabatic case (the second row in Fig. 3) indicates completely GOE trends for both measures. Therefore, as far as we know, this is the first evidence that ''chaos'' can be induced by the nonadiabatic coupling within the pure quantum mechanical scheme. Hence we think that it deserves to be called ''nonadiabatic chaos'' to distinguish it from the chaos studied by Leitner *et al.*

The present paper has been concentrated on the statistical properties of spectra and amplitude distribution of the eigenstates. To clarify the dynamical nature of the present chaos, however, more should be explored. The mechanism and scenario of onset of the chaos needs to be elucidated. In particular, the relationship between the genesis of chaotic eigenfunctions and the dynamics of surface hopping should be clarified [22]. In this regard, our comparative study between the hopping trajectories and the corresponding chaotic eigenfunctions (Figs. 6, 7, and 8 in Ref. [22]) shows that the simple surface-hopping view can well represent the first order feature of the wave functions in an initial stage. However, such an intuitive picture of ''mode mixing'' (chaos) is eventually deteriorated, since the interference effect is essential to produce quantum spectra. To study further, the path-integral methods and/or semiclassical methods must be use-

TABLE II. Characteristics of the TMTS system with the intermediate Duschinsky angle ($\theta=\pi/6$). The other parameters are listed in Table I.

	Lower adiabatic system	Nonadiabatic system
Weak coupling ($J=0.3$)	~mixed	~mixed
Intermediate coupling ($J=1.5$)	~mixed	chaos
Strong coupling ($J=7.5$)	~mixed	~mixed

ful to take account of an interference effect arising from the hopping motions. Also, the kind of nonadiabatic couplings, i.e., the types of avoided crossing and conical intersection, should make a difference. The evolution of the chaotic property in eigenfunctions as a function of the magnitude of the nonadiabatic coupling is a very interesting subject to be studied. We will discuss these aspects in our future publication.

ACKNOWLEDGMENTS

One of the authors (H.F.) thanks Professor A. Shudo and Dr. A. Tanaka for helpful discussions, and Professor V. McKoy for improving this manuscript. This work was supported in part by a Grant-in-Aid from the Ministry of Education, Science, and Culture of Japan.

[1] M. C. Gutzwiller, *Chaos in Classical and Quantum Mechanics* (Springer-Verlag, New York, 1990), and references therein.
[2] M. V. Berry, Proc. R. Soc. London, Ser. A **413**, 183 (1987).
[3] O. Bohigas, M-J. Giannoni, and C. Schmit, Phys. Rev. Lett. **52**, 1 (1984); O. Bohigas, in *Chaos and Quantum Physics*, Proceedings of the LII Session of Les Houches Summer School, 1989, edited by M. -J. Giannoni, A. Voros, and J. Zinn-Justin (Elsevier Science, B. V. 1991).
[4] M. V. Berry, J. Phys. A **10**, 2083 (1977).
[5] E. J. Heller, Phys. Rev. Lett. **53**, 1515 (1984); M. V. Berry, Proc. R. Soc. London, Ser. A **423**, 219 (1989); L. Kaplan and E. J. Heller, Ann. Phys. **264**, 171 (1998).
[6] G. Casati, B. V. Chirikov, F. M. Izailev, and J. Ford, in *Stochastic Behavior in Classical and Quantum Hamiltonian Systems*, edited by G. Casati and J. Ford, Lecture Notes in Physics, Vol. 93 (Springer, Berlin, 1979); S. Fishman, D. R. Grempel, and R. E. Prange, Phys. Rev. Lett. **49**, 509 (1982).
[7] H. Ushiyama and K. Takatsuka, Phys. Rev. E **53**, 115 (1996).
[8] A. Shudo and K. S. Ikeda, Physica D **115**, 234 (1998).
[9] S. Tomsovic and D. Ullmo, Phys. Rev. E **50**, 145 (1994); J. Zakrzewski, D. Delande, and A. Buchleitner, *ibid.* **57**, 1458 (1998).
[10] K. Takatsuka, H. Ushiyama, and A. Inoue-Ushiyama, Phys. Rep. **322**, 347 (1999).
[11] M. V. Berry, Proc. R. Soc. London, Ser. A **400**, 229 (1985).
[12] E. J. Heller, S. Tomsovic, and M. A. Sepúlveda, Chaos **2**, 105 (1992); M. A. Sepúlveda and F. Grossmann, Adv. Chem. Phys. **96**, 191 (1996).
[13] K. Takatsuka and A. Inoue, Phys. Rev. Lett. **78**, 1404 (1997); A. Inoue-Ushiyama and K. Takatsuka, Phys. Rev. A **59**, 3256 (1999); **60**, 112 (1999).
[14] L. Bonci, R. Roncaglia, B. J. West, and P. Grigolini, Phys. Rev. Lett. **67**, 2593 (1991); L. Müller, J. Stolze, H. Leschke, and P. Nagel, Phys. Rev. A **44**, 1022 (1991); K. Furuya, M. C. Nemes, and G. Q. Pellegrino, Phys. Rev. Lett. **80**, 5524 (1998).
[15] P. Grigolini, *Quantum Mechanical Irreversibility and Measurement* (World Scientific, Singapore, 1993).
[16] A. Tanaka, J. Phys. A **29**, 5475 (1996); Phys. Rev. Lett. **80**, 1414 (1998).
[17] P. Meystre and M. Sargent, III, *Elements of Quantum Optics*, 3rd ed. (Springer-Verlag, Berlin, 1998).
[18] H. Kobayashi, N. Hatano, and S. Miyashita, Physica A **265**, 565 (1999).
[19] A. M. Kuznetsov and J. Ulstrup, *Electron Transfer in Chemistry and Biology* (Wiley, New York, 1999); for recent topics, see the articles in Adv. Chem. Phys. **106**, 107 (1999).
[20] K. Takatsuka, Y. Arasaki, K. Wang, and V. McKoy, Faraday Discuss. **115**, 1 (2000).
[21] E. J. Heller, J. Chem. Phys. **92**, 1718 (1990).
[22] H. Fujisaki and K. Takatsuka, J. Chem. Phys. **114**, 3497 (2001).
[23] E. J. Heller, J. Chem. Phys. **72**, 1337 (1980); E. B. Stechel and E. J. Heller, Annu. Rev. Phys. Chem. **35**, 563 (1984).
[24] D. M. Leitner, H. Köppel, and L. S. Cederbaum, J. Chem. Phys. **104**, 434 (1996).
[25] S. W. McDonald and A. N. Kaufman, Phys. Rev. A **37**, 3067 (1988); Y. Shimizu and A. Shudo, Prog. Theor. Phys. Suppl. **116**, 267 (1994).
[26] H. Kupka and P. H. Cribb, J. Chem. Phys. **85**, 1303 (1986); D. Gruner and P. Brumer, Chem. Phys. Lett. **138**, 310 (1987); A. M. Mebel, M. Hayashi, K. K. Liang, and S. H. Lin, J. Phys. Chem. A **103**, 10 674 (1999).
[27] K. Takatsuka and N. Hashimoto, J. Chem. Phys. **103**, 6057 (1995).
[28] W. H. Press, S. A. Teukolsky, W. T. Vetterling, and B. P. Flannery, *Numerical Recipes in FORTRAN, The Art of Scientific Computing*, 2nd ed. (Cambridge University Press, Cambridge, 1992).
[29] H. Fujisaki and K. Takatsuka (unpublished).
[30] W. Karrlein, J. Chem. Phys. **94**, 3293 (1990); F. Pichierri, J. Botina, and N. Rahman, Phys. Rev. A **52**, 2624 (1995).
[31] E. Haller, H. Köppel, and L. S. Cederbaum, Chem. Phys. Lett. **101**, 215 (1983); Th. Zimmermann, H. Köppel, and L. S. Cederbaum, J. Chem. Phys. **91**, 3934 (1989).
[32] M. Kuś, Phys. Rev. Lett. **54**, 1343 (1985).
[33] R. Graham and M. Höhnerbach, Phys. Rev. Lett. **57**, 1378 (1986); in *Quantum Measurement and Chaos*, edited by E. R. Pike and S. Sarkar (Plenum, New York, 1987).
[34] T. Terasaka and T. Matsushita, Phys. Rev. A **32**, 538 (1985); A. Shudo and T. Matsushita, *ibid.* **39**, 282 (1989).
[35] M. V. Berry and M. Tabor, Proc. R. Soc. London, Ser. A **356**, 375 (1977); A. Pandey and R. Ramaswamy, Phys. Rev. A **43**, 4237 (1991); L. Ji-zhi, *ibid.* **49**, 48 (1994).
[36] W. P. Reinhardt, J. Phys. Chem. **86**, 2158 (1982); C. Jaffé and W. P. Reinhardt, J. Chem. Phys. **77**, 5191 (1982); R. B. Shirts and W. P. Reinhardt, *ibid.* **77**, 5204 (1982).